SINGLE-CELL RNA-SEQ OF hPSC-DERIVED NEURAL CELL TYPES REVEALS EARLY GLIA-SPECIFIC DIFFERENTIATION TRAJECTORIES

Vukasin M. Jovanovic, Jaroslav Slamecka, Marissa Hirst, David Gailbraith, Chaitali Sen, Carlos A. Tristan, Pinar Ormanoglu, Ilyas Singeç

National Center for Advancing Translational Sciences (NCATS), Division of Preclinical Innovation, Stem Cell Translation Laboratory (SCTL), Rockville, MD 20850, USA

National Center for Advancing Translational Sciences

COLLABORATE. INNOVATE. ACCELERATE.

Abstract

During brain development, radial glia cells (RGCs) generate neurons first followed by astrogliogenesis, a process known as the "gliogenic switch" of neural lineage progression. While neurogenesis has been extensively characterized, the underlying molecular mechanisms whereby RGCs differentiate into astrocytes remain elusive. Here, we performed single-cell mRNA sequencing (scRNA-seq) of astrocytes derived from human pluripotent stem cells (hPSC) by using a new highly efficient approach that achieves direct RGC-to-astrocyte conversion in the absence of neurogenesis (Jovanovic *et al.,* 2021). The single-cell transcriptome of these directly differentiated astrocytes was then compared to commercially obtained astrocytes and cortical glutamatergic neurons (FUJIFILM CDI). Altogether, we profiled the transcriptomes of 12,771 cells and unbiased clustering identified 11 transcriptionally distinct cell clusters. After data integration with single-cell transcriptomes of the developing human cortex, as expected, cluster signatures corresponded to 3 broad categories: radial glia, astrocytes, and cortical neurons. To better understand cell type-specific molecular identities, we performed slingshot analysis and identified three different trajectories mapping transition of RGCs into two branches representing astrocytes and one "teleporting" RGCs (in the absence of neurogenesis transitional states were not detected) to excitatory neurons. To correlate gene expression variation to each of the cell types in pseudotime, we performed trajectory-based differential expression analysis (trade-Seq) and identified new gene expression modules that characterize the differentiation of RGCs directly into astroglia at the expense of neurogenesis.

Controlled differentiation of hPSCs into radial glia and astrocytes

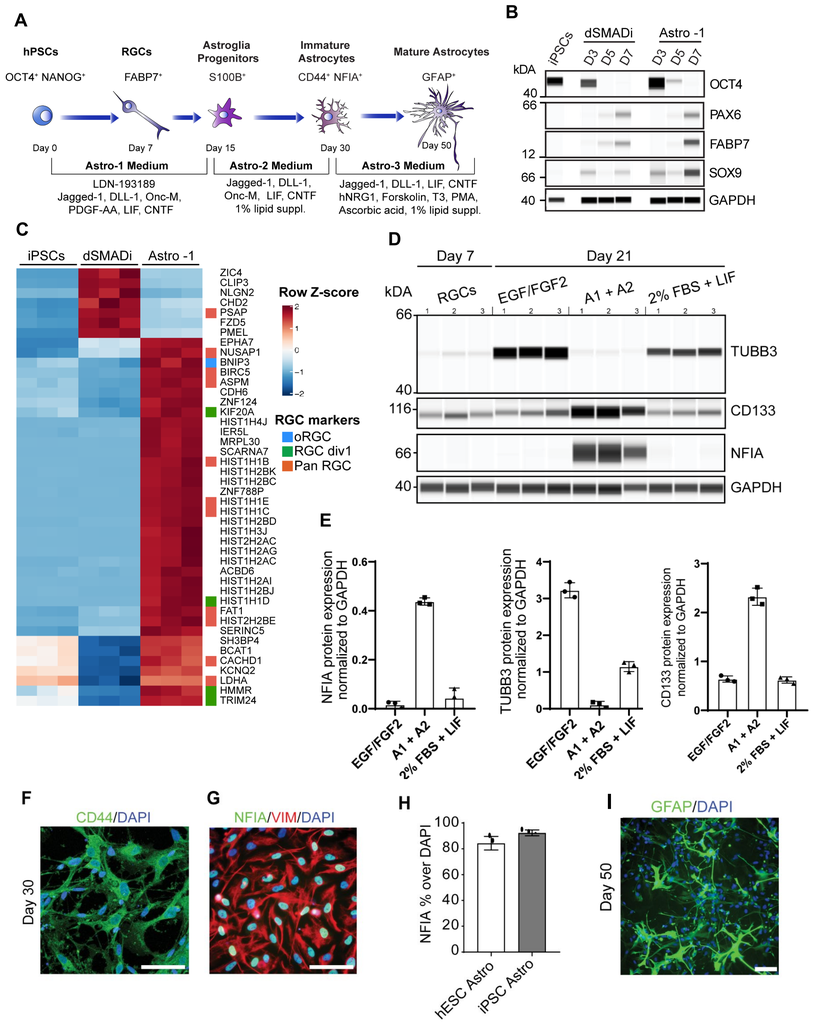

Figure 1. Differentiation of iPSCs into RGCs and astrocytes at the expense of neurogenesis.
(**A**) Schematic illustration depicting RGC and astrocyte differentiation from hPSCs using chemically defined Astro-1, Astro-2, and Astro-3 media.
(**B**) Western blot analysis of OCT4, PAX6, FABP7, and SOX9. See the difference in FABP7 and SOX9 between cultures differentiated with Astro-1 versus dSMADi.
(**C**) Heatmap showing differentially expressed RGC genes after neural induction with dSMADi and Astro-1.
(**D**) Western blot analysis of RGCs (day 7), RGCs treated with from day 7-21 with EGF/FGF2 (25 ng/ml each), Astro-1 and Astro-2 (A1+ A2) or 2% FBS + LIF (10 ng/ml).
(**E**) Quantification of Western blots (normalized to GAPDH, n = 3) for NFIA, TUBB3 (TUJ1), and CD133 protein expression. Note the robustness of NFIA and CD133 upregulation after A1/A2 treatment of RGCs, and the absence of neuronal marker TUBB3 as compared to other conditions.
(**F, G**) Immunocytochemical analysis of astrocyte markers CD44, NFIA, and VIMENTIN (day 30).
(**H**) Quantification of NFIA+ glial cells normalized to total number of nuclei (day 30).
(**K**) Immunostaining showing astrocytes with typical stellate morphologies expressing GFAP (day 50).
Scale bars, 100 µm.
Representative experiments were performed with hESCs (WA09) and iPSCs (LiPSC-GR1.1 and NCRM5) and showed similar results.

Single-cell RNA-seq and comparison of astrocytes and neurons

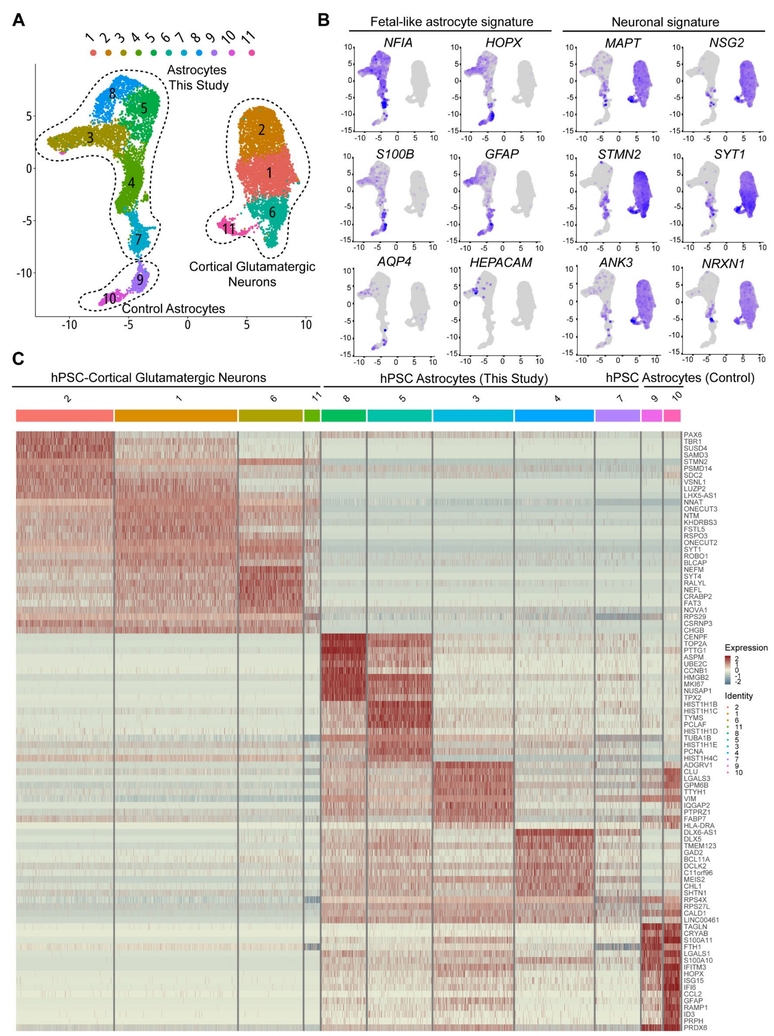

Figure 2. Single-cell profile of hPSC-derived astrocytes as compared to hPSC-excitatory cortical-like neurons.
(**A**) UMAP plot of 12,771 hPSC-derived neural cells showing 11 distinct cell clusters. Clusters are color-coded and dotted lines demarcate different cell types.
(**B**) Feature plots for genes common across fetal and adult astrocyte subtypes and postmitotic neurons.
(**C**) Gene expression heatmap for the top-10 genes expressed across clusters. Rows correspond to genes, columns to cells/clusters. Blue/yellow, low gene expression; Red, high expression. Note the clear difference between neuronal and astrocyte signatures.

Single cell transcriptome of hPSC-astrocytes and comparison to cell types of human fetal cortex

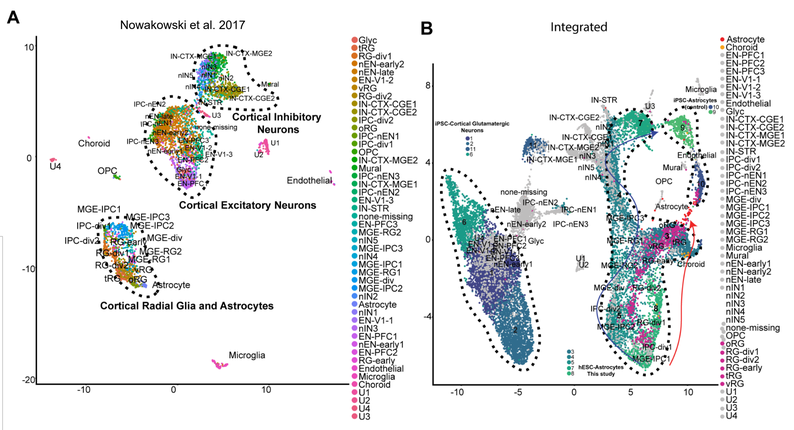

Figure 3. Data integration with fetal cortex implies bi-directional RGC differentiation into astrocytes.
(**A**) UMAP plot of 4,261 cells from the Nowakowski et al. (2017), sampled across the human cortex development (gestational week 5-37) outlines three broad clusters excitatory neurons, inhibitory neurons, and radial glia/astrocyte. (**B**) UMAP showing integration of hPSC-derived astrocytes (this study) and cortical excitatory neurons (Nowakowski et al., 2017). Due to the differences in the number of profiled cells the hPSC cluster size was significantly larger. Note that hPSC-astrocytes cluster together with radial glia /astrocytes.

Pseudotime trajectory analysis identifies new astrocyte markers

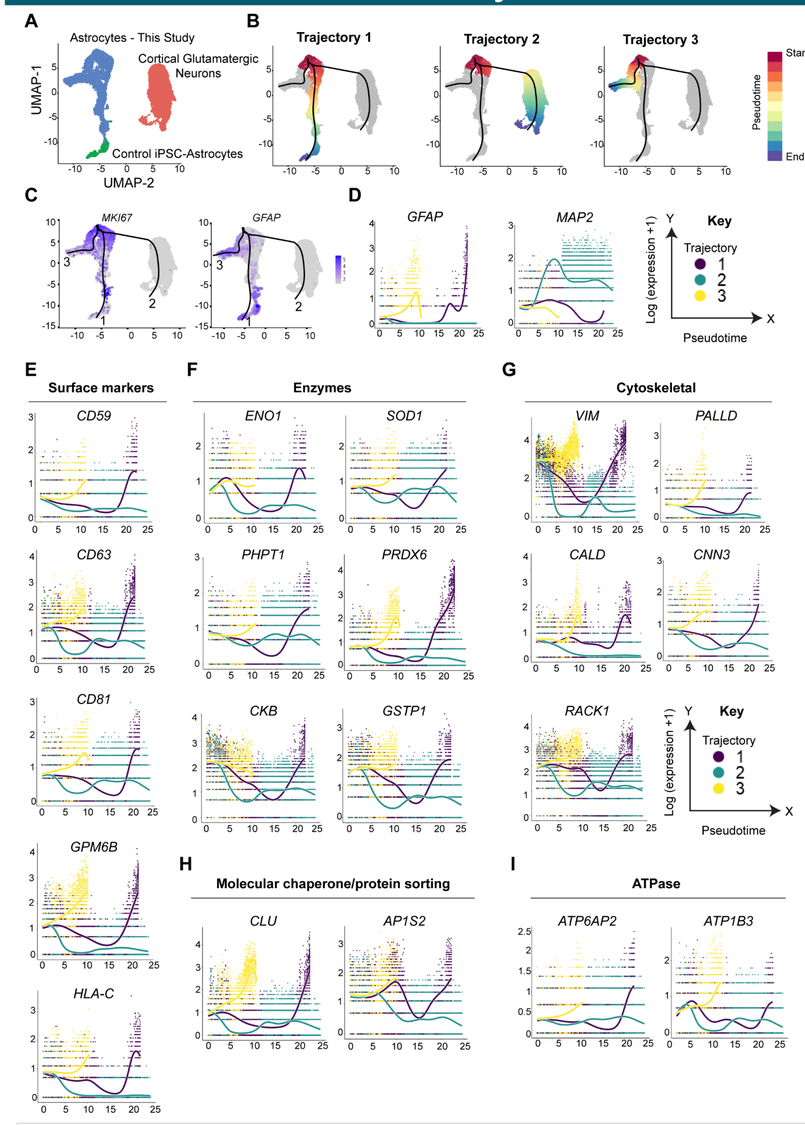

Figure 4. Characterization of astrocyte differentiation.
(**A**) UMAP plot of 12,771 hPSC-derived neural cells color-coded by cell type. Blue-astrocytes generated in this study; Green-control astrocytes (FUJIFILM CDI); Red-cortical glutamatergic neurons (FUJIFILM CDI). (**B**) Slingshot analysis maps 3 different trajectories of cell progression. Red-pseudotime start point, blue-pseudotime end point. (**C**) Feature plots for MKI67 and GFAP genes. Note that all pseudotime trajectories start in the clusters with high MKI67 and low GFAP expression and progress to areas with high GFAP expression (1 and 3) or no GFAP expression (2, neurons). (**D**) Analysis of gene expression dynamics relative to the previously identified trajectories performed using trade-Seq shows GFAP induction along trajectories 1 and 3 (astrocytes) and MAP2 induction along trajectory 2 (neurons). (**E-I**) Gene expression of surface markers, enzymes, cytoskeletal proteins, molecular chaperones, and ATPases identified astrocyte-specific markers. Note that many of these genes are implicated in neurodegenerative diseases (e.g., SOD1, CLU, ATP6AP2).

Conclusions

- Directed differentiation of hPSC under chemically-defined conditions provides unique opportunities for better understanding the molecular underpinnings of RGC-to-astrocyte transition, cellular diversity, and astrocyte maturation in the absence of neurogenesis and the gliogenic switch.
- Detailed analyses provide new insights into RGC biology, glia-specific differentiation, and identifies new markers with relevance for brain diseases.

References

1. Jovanovic, V.M., Malley, C., Tristan, C.A., Ryu, S., Chu, P.-H., Barnaeva, E., Ormanoglu, P., Mercado, J.C., Michael, S., Ward, M.E., et al. (2021). Directed Differentiation of Human Pluripotent Stem Cells into Radial Glia and Astrocytes Bypasses Neurogenesis. bioRxiv, 2021.2008.2023.457423. 10.1101/2021.08.23.457423.

2. Nowakowski, T.J., Bhaduri, A., Pollen, A.A., Alvarado, B., Mostajo-Radji, M.A., Di Lullo, E., Haeussler, M., Sandoval-Espinosa, C., Liu, S.J., Velmeshev, D., et al. (2017). Spatiotemporal gene expression trajectories reveal developmental hierarchies of the human cortex. Science 358, 1318-1323. 10.1126/science.aap8809.

3. Street, K., Risso, D., Fletcher, R.B., Das, D., Ngai, J., Yosef, N., Purdom, E., and Dudoit, S. (2018). Slingshot: cell lineage and pseudotime inference for single-cell transcriptomics. BMC Genomics 19, 477. 10.1186/s12864-018-4772-0.

4. Van den Berge, K., Roux de Bezieux, H., Street, K., Saelens, W., Cannoodt, R., Saeys, Y., Dudoit, S., and Clement, L. (2020). Trajectory-based differential expression analysis for single-cell sequencing data. Nat Commun 11, 1201. 10.1038/s41467-020-14766-3.

Funding: NIH Common Fund (OD); NCATS Intramural Research.